JOURNAL OF APPLIED ELECTROCHEMISTRY **28** (1998) 337–342

Electrodiffusional flow diagnostics in a centrifugal pump*

M. LUTZ, V. DENK

Lehrstuhl für Fluidmechanik und Prozeßautomation, Technische Universität München, D-85350 Freising, Germany

K. WICHTERLE, V. SOBOLÍK

Institute of Chemical Process Fundamentals, Academy of Sciences of the Czech Republic, CZ-16502 Prague 6, Czech Republic

Received 14 February 1997; revised 10 March 1997

This paper presents electrodiffusional measurements of the wall shear rate at the impeller surface of a radial centrifugal pump. Twelve probes of different radii and at different positions along one blade were used in a pump with an open six bladed impeller. By means of throttling and speed control the operating point of the pump was adjusted and the influence on the wall shear rate was studied. The measurements were related to the analytical solution for a free rotating disc and the shear gradients were in the same order of magnitude.

Keywords: *electrodiffusion*, *flow measurements*, *centrifugal pump*, *shear rate*, *soft processing*, *open impeller*

List of symbols

H	head (m)
I	current (A)
d	diameter (m)
n	rotational speed (s^{-1})
P	power input (W)
$\dot{Q}$	flow rate ($m^3 s^{-1}$)
r	radius (m)
s	gap width (m)
Re	Reynolds number
T	temperature (K)
v	velocity ($m s^{-1}$)

Greek symbols

$\dot{\gamma}$	shear rate (s^{-1})
φ	delivery coefficient
ν	kinematic viscosity ($m^2 s^{-1}$)
τ	shear stress (Pa)
ω	angular velocity ($rad s^{-1}$)

Subscripts

L	local
r	radial
u	circumferential

1. Introduction

Centrifugal pumps are widely used for the transportation of liquids with shear sensitive properties, for example, in the food industry and other biotechnological or chemical processes. To prevent these materials from being damaged, great attention has to be paid to local shear stresses. Even though the pump-manufacturers claim that their pumps handle liquids benignly, actual shear stresses in centrifugal pumps are yet unknown.

The flow inside a pump has been investigated by means of laser–Doppler–velocimetry for the characterization of the main flow patterns and the turbulent shear forces in the fluid [1]. To support this optical method in regions close to walls, we use electrodiffusion probes for measurement of the wall shear rate in order to get a complete representation of the flow conditions inside the pump.

In this paper results of wall shear rate measurements at the impeller surface are presented, where the most significant wall shear stresses are expected to arise. Because the sensitivity of mechanical shear stress sensors is low, direct measurement of the shear stress is difficult. Electrodiffusion diagnostics is an efficient method for the measurement of wall shear stress rates and it was applied to a rotating centrifugal pump impeller up to speeds of 2850 rpm. Shear stress can be calculated from the shear rate by means of the viscosity function.

*This paper was presented at the Fourth European Symposium on Electrochemical Engineering, Prague, 28–30 August 1996.

0021-891X

2. Experimental details

2.1. *Electrodes, solution, calibration*

Measurements of wall shear rates at the surface of an impeller blade were carried out using twelve circular platinum probes, each with a diameter d of about 0.5 mm. Four probes were glued on the pressure side, three on the suction side and three on the tip of one impeller blade. One probe was located in the channel between two blades and one on the rear side of the impeller. The positions of the probes are shown in Fig. 1.

Six probes at a time were connected using slip rings to a six channel electrodiffusional interface. The stainless steel impeller shaft served as the auxiliary electrode and the well known ferri-, ferrocyanide system (concentration $c = 10\,\mathrm{mol\,m^{-3}}$) with potassium sulfate (2%) as supporting electrolyte in demineralized water. To prevent the probes from being polluted, great attention was paid to all parts of the pump test rig which was made of stainless steel and PVC only.

Data acquisition and experiment control of the wall shear measurements were done by means of a PC with an A/D and D/A board. The signals on the platinum probes lay in the range 10–150 μA. Due to the geometry of the impeller it was not possible to perform a calibration of the probes in a well defined shear flow (e.g., Couette flow). Therefore, the 'voltage-step transient' experiment [2] had to be used to determine the proportionality constant k for the calculation of the actual shear rates $\dot{\gamma}$ from the measured electric current I:

$$\dot{\gamma} = kI^3 \tag{1}$$

Additionally, the voltage-step transient experiment has the advantage that it is highly sensitive to the working conditions of the wall shear probes. This method was therefore repeated after each series of measurements. Thus, a repeatability of the measurements better than 10% was achieved and for the absolute value of the shear rate on the wall an accuracy better than 20% is a realistic assumption.

2.2. *Pump and test rig*

A centrifugal pump with an open impeller of $d = 176\,\mathrm{mm}$ diameter was used. The impeller was mill-cut out of synthetic material. The pump test rig contained a total volume of about $65\,\mathrm{dm^3}$ of electrolyte and provided a straight inlet section to the pump of $40\,d$ and an outlet section of $25\,d$ (Fig. 2). The usual complete characteristics including temperature T, flow rate $\dot{Q}$, head H, rotational speed n, and power input P were measured simultaneously for the determination of the operating point of the pump.

In these experiments an additional pressure of nitrogen on the whole system was used to raise the existing net positive suction head (NPSH) of the installation. For the highest rotational speeds, above 2000 rpm, it was not possible to investigate the whole characteristic curve because of cavitation in the throttle.

Two kinds of experiments were performed. One was, to run the pump with constant rotational speed and vary the flow rate with the additional resistance of a throttling valve (throttling control). The other

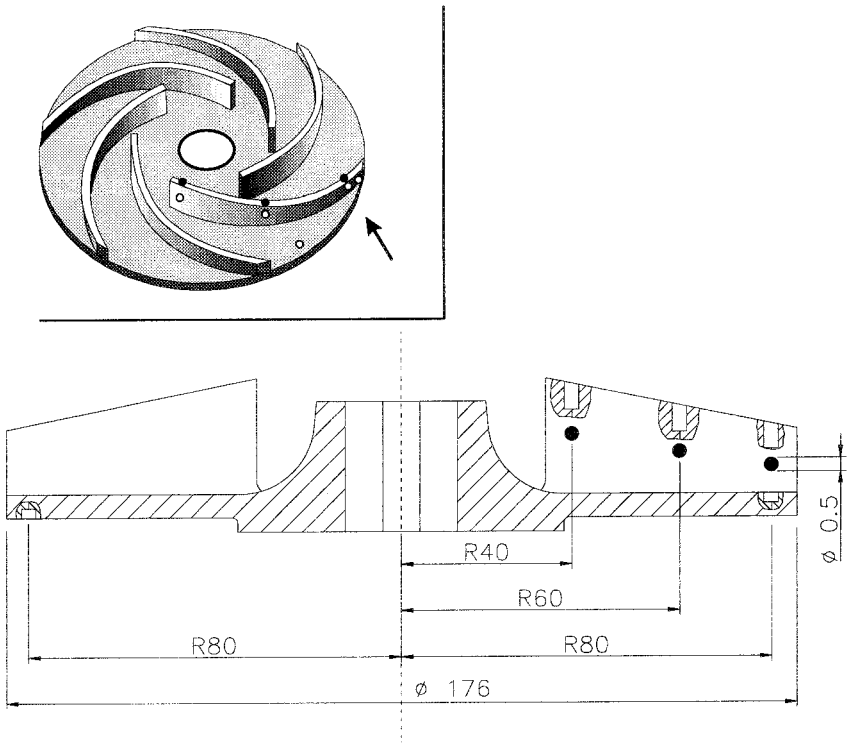

Fig. 1. Impeller geometry and positions of the electrodes.

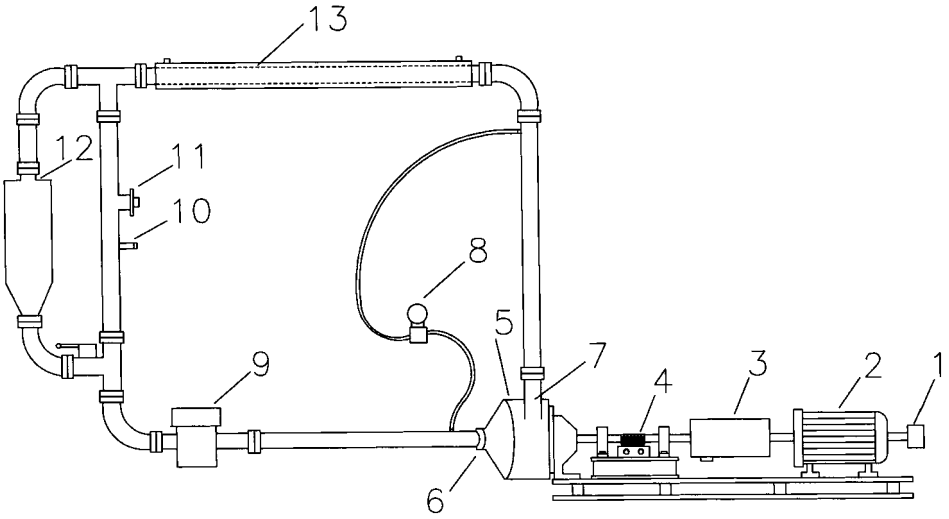

Fig. 2. Schematical sketch of the pump test rig. Key: (1) shaft encoder, (2) motor, (3) torque metering hub, (4) sliding contacts, (5) pump casing, (6) suction branch, (7) pressure branch, (8) pressure measurement, (9) flowmeter, (10) temperature measurement, (11) throttle, (12) compensation tank and (13) cooler.

was to change the rotational speed of the impeller at a fixed position of the throttle (speed control). Thus, a variety of pump operating conditions were investigated. The temperature was kept constant at $T = 20\,^{\circ}\mathrm{C}$ and rotational speeds reached 2850 rpm, which is equivalent to the speed of commonly used double pole asynchronous motors. The pump casing was identical to an industrially used casing, but made out of glass in order to observe cavitation and to be sure the whole system was without any air inclusions. Inlet and outlet diameters of the pump were $d = 50\,\mathrm{mm}$. The specific speed of the pump at its point of best efficiency was $n_q = 27\,\mathrm{min}^{-1}$.

The pump was operated at flow rates up to $\dot{Q} = 38\,\mathrm{m}^3\,\mathrm{h}^{-1}$ and a maximum head of $H = 12\,\mathrm{m}$ water column. The maximum efficiency was only $\eta_{opt} = 0.42$, due to the large gap between the blades and the casing ($s \approx 10\,\mathrm{mm}$).

3. Results and discussion

3.1. *Wall shear rates at the impeller*

A typical result for a measurement with six probes at constant rotational speed (1450 rpm) over the whole characteristic curve is shown in Fig. 3. It is clear that the wall shear rates inside the impeller depend on the flow rate through the pump, the radial position of the probe, its position on the blade ('pre' indicates pressure side, 'suc' the suction side and 'pass' the passage between two blades) and of the rotational speed of the impeller. With higher flow rate, the radial component of the fluid velocity increases and so does the shear rate in the boundary layer. Values of the wall velocity gradient up to $1.8 \times 10^5\,\mathrm{s}^{-1}$ were measured. The shear rate on the suction side is higher than on the other sides of the blades and the ratio stays almost constant (at $r = 80$: suc/pre ≈ 1.5) for the flow rates investigated. Values in the passage between two blades are lower than on the blades at the same radius for all impeller speeds. At the outer edge of the impeller, at a radius of $r \geqslant 80\,\mathrm{mm}$, the wall shear rate remains constant for flow rates approaching zero. Under these circumstances, the circumferential velocity ($\bar{v}_u$ of the impeller $\approx 12.5\,\mathrm{m\,s}^{-1}$) becomes dominant and the influence of the radial velocity component, which is proportional to the flow rate, is no longer detectable.

This is probably an effect of the large gap between the blades and the casing in this area. There is much space for the fluid in front of the impeller which leads to low fluid velocities and high relative movement compared to the impeller. This results in secondary flows over the blades which exceed the influence of the comparatively small radial component.

At a radius of 40 mm at the inlet of the impeller, the wall shear rate shows a linear increase over the whole characteristic curve at this impeller speed, a result of different geometrical conditions at this radius: namely,

(i) the circumferential velocity of the impeller is significantly lower ($\bar{v}_u \propto r\,n$), and the radial velocity at the inlet is higher than at the impeller

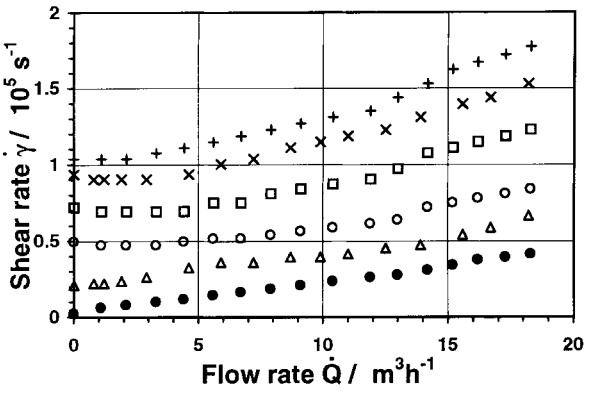

Fig. 3. Shear rates at the impeller surface at different positions (1450 rpm). Probe positions/mm: (+) r80 suc; (×) r85 pre; (□) r80 pre; (○) r80 pass; (△) r60 suc; (●) r40 suc.

edge because of the enlarging cross section ($\overline{v}_r \propto \dot{Q}/A \propto 1/r$);

(ii) the gap is smaller than at the outer region of the impeller and therefore the dependent secondary flows are of less influence; and

(iii) because of the 90° turn of the axial inflow to the radial outflow direction, most of the fluid flows *inside* the impeller between the blades and therefore affects the near wall conditions even at low flow rate.

3.2. *Comparison to a free rotating disc*

An obvious possibility for an evaluation of the shear rates at the impeller wall is comparison to the analytical solution for the wall shear rate on a rotating disc in a 'free' fluid [3, 4].

According to the theory of Kármán the shear rate in the laminar boundary layer ($Re_L \leqslant 2 \times 10^5$) on the disc in a Newtonian liquid is

$$\dot{\gamma}_{disc} = 6.302\sqrt{Re_L} \times n \tag{2}$$

where the local Reynolds number Re_L for points on the radius $r = d_L/2$ is defined as

$$Re_L = \frac{nd_L^2}{v} \tag{3}$$

A comparison of the data with Equation 2 is shown in Fig. 4, again for 1450 rpm. The dimensionless delivery coefficient

$$\varphi = \frac{\dot{Q}}{nd^3} \tag{4}$$

is a useful number for comparing different pumps. It is calculated using the diameter of the impeller.

The measured values of the shear rate are all in the same range as predicted for the free disc. But, because the impeller can be considered to be a disc in a housing (as mentioned, the ratio of gap width s to radius is about $s/r \approx 0.2$ in front of the impeller), it is obvious that the detected shear rates are lower than expected according to Equation 2 for most of the measurements. The bulk fluid surrounding a disc in a housing is corotating with an angular speed of approximately half the disc speed and so the velocity gradients are between 0.5 and 0.7 of the values predicted for the free disc [4]. Again, the small influence of the flow rate at the outer radius for low φ values is demonstrated and the related shear rates on the impeller surface show almost constant values. Higher flow rates lead to secondary flows over the blades and the related shear rates exceed the values predicted by Equation 2. At low flow rates, the fluid seems to be corotating with almost the impeller speed at the blade inlet and the related shear rates reach only 10% of the free disc values.

The impeller back side represents a disc in a closed casing with a gap of about 50 mm which leads to a ratio s/r of 0.57. Even if this value exceeds the limit of known measurements with discs, there should still be some similarity. Thus the shear rates measured at this position depend only on the rotational rate, $\dot{\gamma} \propto n^{3/2}$, and, as mentioned above, the values of the local velocity gradients should be about half the free disc values [4]. The data in Fig. 4 show good consistency with the analytical solution. Because no dependence on the flow rate was found the probe on the back side of the impeller is useful for evaluation of the working conditions of the electrodiffusion measurements.

3.3. *Reynolds number dependence of related shear rates*

Figure 5 shows the dependence of normalized shear rate on the local Reynolds number Re_L. To minimize the effect of changing flow rate (which is, of course, linearly related to the rotational speed), only data of comparatively low delivery coefficients φ are used. The shear rates show a dependence on the rotational speed of $\dot{\gamma} \propto n^{3/2}$, for Reynolds numbers up to $Re_L \approx (3\text{–}4) \times 10^5$ (validity of the laminar Kármán solution: $Re_L \leqslant 2 \times 10^5$) and a steeper increase for higher Reynolds numbers. This seems to result from turbulent conditions in the boundary layer. The absolute value of the wall shear rates depends not

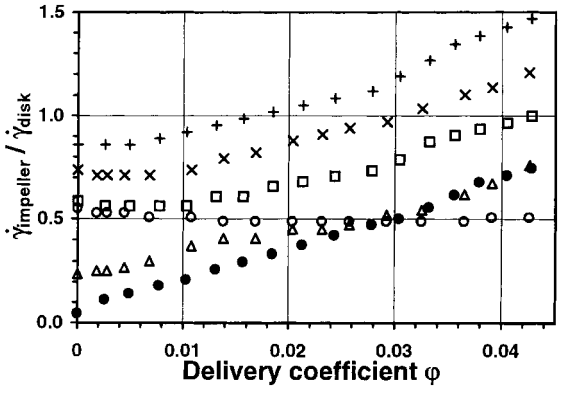

Fig. 4. Related shear rates on the impeller against dimensionless flow coefficient φ (1450 rpm). Probe positions/mm: (+) r80 suc; (×) r85 pre; (□) r80 pre; (○) r80 back; (△) r60 suc; (●) r40 suc.

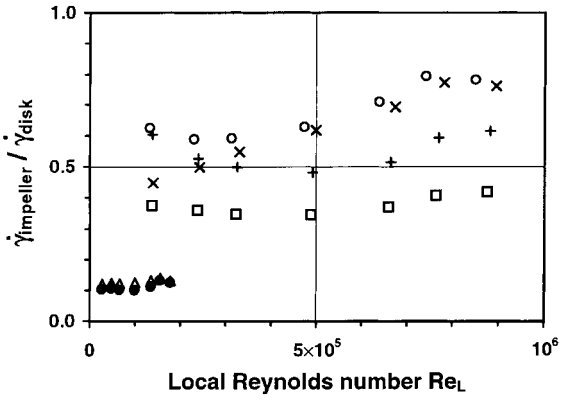

Fig. 5. Related shear rates on the impeller for varying rotational speed against Re_L (low flow rate, $0.002 \leqslant \varphi \leqslant 0.003$). Probe positions/mm: (○) r80 suc; (+) r80 pre; (×) r80 tip; (□) r80 pass; (△) r40 pre; (●) r40 suc.

mainly on the Reynolds number, but on the radial position of the probe, probably due to secondary flows.

At higher flow rates (Fig. 6), the increase in the normalized shear rate begins at lower Reynolds numbers. Turbulence in the boundary layer develops earlier because of the increasing radial flow component ($\overline{v}_r \propto \dot{Q}$, $Re \propto n$). Another effect of high flow rate is observed at $r = 80$. Compared to the pressure side and the tip of the blade, the highest shear rates always appear on the suction side, probably an effect of turbulence due to separation. In laser–Doppler investigations of a similar pump geometry, secondary flows over the blades led to an area of recirculation and high turbulence intensity at the suction side of the blades. As shown, this also affects the boundary layer flow.

At $r = 40$, at the inlet edge of the blade, the conditions mentioned above lead to a large influence of the flow rate, even for very low Re_L. Because this was not detectable for low delivery coefficients ($\overline{v}_r \ll \overline{v}_u$), a comparison with Fig. 5 shows the influence of the flow rate at this radius.

For the characterization of the conditions at higher Reynolds numbers the measured shear rate was normalized by $n\,Re_L$. This dimensionless group is constant if $\dot{\gamma} \propto d_L^2 n^2$ and this dependence is close to the boundary layer theory, according to which $\dot{\gamma} \propto d_L^{8/5} n^{9/5}$ [4]. For high Reynolds numbers, as in industrial pumps, Fig. 7 shows that the normalized shear rate at the wall no longer depends on the Reynolds number, as expected for turbulent conditions.

3.4. *Deduction of wall shear rate out of pump and flow properties*

The flow through the impeller of a centrifugal pump must be considered as a combination of two different influences:

(i) the rotating impeller, similar to a disc in a housing, with a dependence of the shear rate on the rotational speed and the radial position;

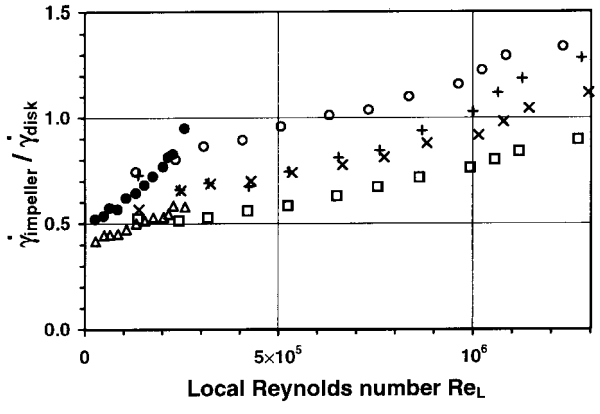

Fig. 6. Related shear rates on the impeller for varying rotational speed against Re_L (high flow rate, $0.03 \leqslant \varphi \leqslant 0.05$). Probe positions/mm: (○) r80 suc; (+) r80 pre; (×) r80 tip; (□) r80 pass; (△) r40 pre; (●) r40 suc.

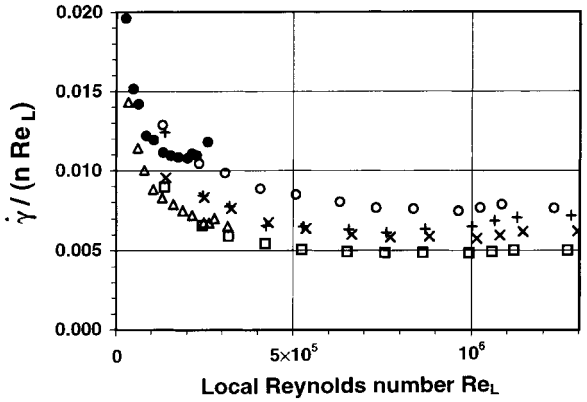

Fig. 7. Normalized shear rate against Re_L. Probe positions/mm. (○) r80 suc; (+) r80 pre; (×) r80 tip; (□) r80 pass; (△) r40 pre; (●) r40 suc.

(ii) the flow through the passages between the blades dependent on the capacity of the pump and the geometry of the impeller.

To take both influences into account, Fig. 8 shows the normalized shear rate versus the delivery coefficient, φ, for the whole system characteristics at different rotational speeds (as indicated for probe r80 suc). For a fully developed turbulent flow in the boundary layer (speed $\geqslant$ 1450 rpm) all data fit a single curve. Therefore, it is possible, to calculate the maximum wall shear stress at this impeller at different rotational speeds and pump capacities. With further electrodiffusional measurements in other pump configurations it might be possible to deduce the apparent wall shear rates from centrifugal pump geometry and operating conditions only. It will also be of interest to examine the difference of open and closed impeller geometries and to minimize secondary flows over the blades using a smaller distance between impeller and front cover of the casing.

3.5. *Adjustment of the operating point*

For operating a pump at varying flow rates, a throttle which means an additional resistance in the pipe system, or a speed control of the pump motor can be

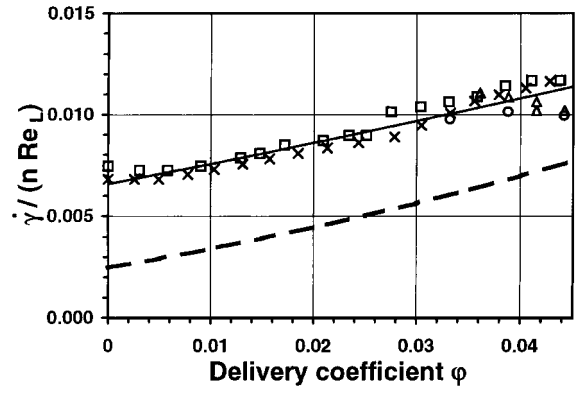

Fig. 8. Related shear rate against delivery coefficient at different rotational speeds. Speed/rpm: (○) 2850; (△) 2500; (□) 2000; (×) 1450; (—) r80 suc; (- - -) r60 suc.

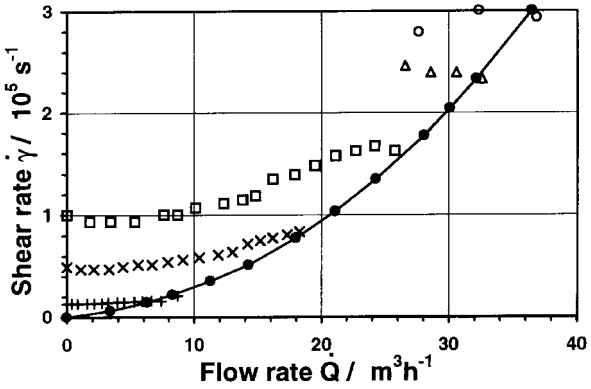

Fig. 9. Comparison of throttling and speed control. Wall shear rate against flow rate at different rotational speed. Probe position: r80 passage. Key, (–•–) speed control, (○) 2850, (△) 2500, (□) 2000, (×) 1450, (+) 720 rpm.

used. The examination of the main flow patterns in the centrifugal pump with the laser–Doppler–velocimeter showed a strong increase in turbulent shear stress due to throttling control in comparison to a speed controlled operation [1].

A similar effect is detectable for the boundary layer flow. Figure 9 displays the wall shear rate, at different flow rates and rotational speeds, measured with the probe in the channel between two blades. For the speed controlled pump operation the wall shear rate decreases with n^2 according to the dependence mentioned above.

Throttling control at constant rotational speed leads at first to a linear decrease in wall shear rate, but at lower flow rates the circumferential velocity becomes dominant and the shear rate reaches a plateau. Thus, the wall shear rate remains significantly higher in the case of the part-load operation of the pump due to throttling control, which is obviously associated with greater energy dissipation. This can lead to differences in the wall shear stress of several hundred pascal, even with the low viscosity of aqueous solutions. This is important for shear sensitive media in biotechnology, since values of the shear stress $\tau \leqslant 50\,\mathrm{Pa}$ may lead to severe product damage.

4. Conclusions

Shear rates at an open pump impeller rotating in a glass housing were measured using twelve embedded electrodiffusional probes of diameter 0.5 mm. The experiments were carried out with speed control (0–2850 rpm) and throttling control of the pump. Shear rates as high as $3 \times 10^5\,\mathrm{s}^{-1}$ were measured. The contributions to the shear rate of the flow around the impeller as a rotating disc and the passage of liquid between the impeller blades were distinguished. There was good agreement between the analytical solution for a free rotating disc and the measurements. The shear gradients on the impeller were of the same order of magnitude and did not exceed the factor of 1.6 times the shear rate calculated from the Kármán laminar boundary layer theory for a rotating disc. The shear rate was proportional to $n^{3/2}$ in the laminar boundary layer, $Re_L \leqslant 3 \times 10^5$, and $\dot{\gamma} \propto n^2$ in the turbulent boundary layer. The normalized shear rate, $\dot{\gamma}/(n\,Re_L)$, was a function of the delivery coefficient, $\varphi = \dot{Q}/(n\,d^3)$, in the turbulent boundary layer. Throttling control of the flow rate was associated with much higher shear rates at the impeller than speed controlled operation. It is possible to make a quantitative estimation of the shear stress for a certain geometry and operating point of a centrifugal pump.

Acknowledgements

The authors wish to acknowledge the following grants: the Arbeitsgemeinschaft Industrieller Forschungsvereinigungen (AiF) (Cologne, grant no. 10423N); the Wissenschaftsförderung der Deutschen Brauwirtschaft e.V. (Bonn) and Philipp Hilge GmbH (Bodenheim/Rhein).

References

[1] M. Lutz, V. Denk and A. Delgado, 'LDA-investigations on turbulent shear stress in a full scale centrifugal pump'. Proceedings of the 8th International Symposium on Applications of Laser Techniques to Fluid Mechanics, Lisbon (1996), pp. 8.1.1–8.1.6.

[2] V. Sobolík, J. Tihon, O. Wein and K. Wichterle, 'Calibration of electrodiffusion friction probes using a voltage-step transient'. Proceedings of the 4th European Symposium on Electrochemical Engineering, Prague (1996).

[3] K. Wichterle, V. Sobolík, M. Lutz and V. Denk, *Chem. Engng Sci.*, **51** (23) (1996) pp. 5227–8.

[4] H. Schlichting, 'Grenzschicht-Theorie', Karlsruhe (1982).